Bull. Astr. Soc. India (2003) **31**, 141–151

Spectroscopic Studies of Solar Corona During Eclipses and with Coronagraph

Jagdev Singh*
Indian Institute of Astrophysics, Bangalore 560 034

Abstract. The profiles of forbidden lines in the coronal spectrum contain information on the physical parameters such as temperature, turbulence, mass motion and density of coronal structures. The spectra of Fe x (6374 Å) emission line during the eclipses revealed that non-thermal velocity of the order of $20 - 30 \mathrm{kms}^{-1}$ need to be invoked to explain the observed excess line widths. We have obtained spectrographic observations of several coronal structures at the solar limb overlying sunspot regions with the 25-cm coronagraph in Fe x (6374 Å) and Fe xi (7892 Å) emission lines on several days and simultaneously in three coronal emission lines 6374 Å [Fe x], 10747 Å [Fe xiii] and 10798 Å [Fe xiii] on some other days. The combination of Fe xiv (5303 Å) and Fe x (6374 Å) emission lines was also chosen for making observations. The slit width of 160 microns provided a spatial resolution of 4″ and a spectral resolution of 77 mÅ at [Fe xiv], 128 mÅ at [Fe x] and 291 mÅ at the [Fe xiii] lines. The width, intensity and Doppler shift of all these lines were computed using Gaussian fits to the observed line profiles. The FWHM of [Fe x] emission line increases at an average rate of 1.24 mÅ/arcsec, 0.55 mÅ/arcsec for [Fe xi], 0.29 mÅ/arcsec for [Fe xiii] and −0.66 mÅ/arcsec for [Fe xiv] lines. These values are inversely correlated with the corresponding ionization temperature for these emission lines. We find that the FWHM of emission lines in coronal structures increases with height if the associated ionization temperature is less than 1.6×10^6 K with the gradient depending upon the ionization temperature of the line and decreases for those greater than 1.6×10^6 K. It implies that it may not always be possible to interpret the observed increase in FWHM with height in terms of an increase in non-thermal velocity, and hence rules out the existence of waves in steady coronal structures.

Keywords : Corona – forbidden emission lines – line-widths

*e-mail:jsingh@iiap.ernet.in

1. Introduction

Detailed information on the physical characteristics of the solar corona can be obtained from the studies of profiles of forbidden emission lines in the spectrum observed during a total solar eclipse or with a coronagraph. They permit us to determine the spatial distribution of kinetic temperature and the influence of turbulent velocities that contribute to the enhanced broadening of the line profile. The study of variations in the line profiles of coronal structure as a function of time can give clues on the dynamical and physical nature of the corona. Slitless evaluations of line profiles using Fabry-Perot interferograms pioneered by Jarrett & von Kluber (1955, 1961) have been used at subsequent eclipses by Delone & Makarova (1969, 1975), Marshall & Henderson (1973), Liebenberg, Bessey & Watson (1975), Bessey & Liebenberg (1984), Chandrasekhar et al. (1991) and Raju et al. (1993) to investigate the temperature and velocity structure of solar corona. The Febry-Perot instrumentation has the advantage of simultaneous registration of fringes over most of corona, from which line profiles can be evaluated, but has the disadvantage of the uncertainty of the contribution by Doppler-shifted elements to the line profile and non-linear dispersion especially for inner fringes. Livingston & Harvey (1982), Singh, Bappu & Saxena (1982) and Singh (1985) have used the multi-slit technique to obtain emission line profiles during total solar eclipses to study the flow and temperature structure of solar corona. Observations obtained during total solar eclipses have the advantages that coronal emission line profiles are almost free from photospheric scattered light but have the disadvantage of short duration. One can observe for long durations using a coronagraph but with photospheric scattered light component in the observed line profiles. The recent development in technology in the CCD cameras and their availability has made it possible to remove the contribution of the phtospheric scattered light and to determine the emission line profiles with high photometric accuracy.

Doyle, Banerjee & Perez (1998) interpreted the increase in FWHM of Si VIII line above the limb due to undamped radially propagating Alfvén waves. From the observations of line widths in transition region Mariska, Feldman & Doschek (1978) have predicted the existence of Alfvén or accoustic waves propagating without dissipation in the solar corona. To determine the physical and dynamical conditions in steady coronal structures we have obtained line profiles over a two or three dimensional coronal region in two coronal emission lines simultaneously on a number of days. The variations in observed FWHM of the emission lines in different parts of coronal structures give clues to the changes in temperature, microturbulence and physical conditions in the coronal strcuture. The observational results are discussed in terms of the evolution of coronal structures, their role in the heating of the solar corona and existence of propagating Alfvén or accoustic waves. Due to lack of space here we discuss the results of the green and red lines only which show extreme variations, other lines follow inbetween behavior.

2. Observations and Data Analysis

Multislit spectroscopy and Fabry-Perot experiments were performed during the total solar eclipse of 1980, 1983, 1994 and 1995 by many obervers, the details of the experiments can be seen in Singh and Cowsik (1997) and references therein. Here we give the summary of observations

made in two emission lines simultaneously on several days using 25-cm coronagraph of Norikura Observatory.

The Coude-type coronagraph and large focus spectrograph permit us to mount two CCD cameras, one at the Littrow focus and the other at that part of the diffracted beam from the grating which over spills the camera mirror. More details about the instrumental setup can be seen in Singh et al. (1999, 2002, 2003). A slit width of 160 microns used for observations, correspond to 4″ on the solar iamge and 77 mÅ and 128 mÅ at the green (4th order) and red line (3rd order) spectra, respectively. A faster scan at 50 successive locations in the solar corona in steps of 4″ and exposure time of 10 s for each position could be completed in about 10 m.

The image scale of the obtained spectra is 2.25″ and 2.09″ per pixel for the red and green lines, respectively. Though spectral resolution is 31.8 mÅ per pixel for the green line and 58.5 mÅ for the red line, the large slit width reduces the overall resolution of the spectra. Each spectrum has been corrected for the dark current, pixel-to-pixel sensivity variation and the scattered light component due to sky brightness.

A Gaussian fit was made to the observed emission line profile at each location of the observed coronal region and at different times to compute its peak intensity, central wavelength and width of the emission line. These values were then plotted as a function of spatial locations to obtain spectroheliograms, velocity-grams and width-grams of the selected coronal region in the coronal lines. The heliograms, which have different scales due to different effective focal lengths of the optics used to image the spectra, were re-scaled and brought on the same spatial scale and dimensions using the solar disc spectrum obtained with three fiducial marks made by three wires in front of the entrance slit of the spectrograph.

Top panel of the Figure 1 shows a typical observed line profile for the red coronal emission line. In the bottom panel of the figure we have plotted the residual data after doing the flat field correction and substracting the scattering light component due to sky brightness. The computed Gaussian curve to the residual data plotted over it indicates a good fit. Most of the time a single Guassian fit to the observed emission line profile was found to be satisfactory; at no instance the observed line profiles showed double peaks. The intensity, line-of-sight and line-wdith distributions are shown in the top, middle and bottom panels of Figure 2 respectively.

To begin with all the coronal structures visible in the observed region were considered together and the line-widths, relative intensities and velocities were computed to see the general trend in these parameters. We have selected 200 locations with a resolution of 4″ × 4″ on various coronal structures visible in the red line images. The corresponding locations in other images were selected automatically using software. Similarly we have done the analysis for individual open and closed coronal structures by selecting 15–20 locations depending upon the length of the individual structure to investigate the physical differences between these two kinds of structures.

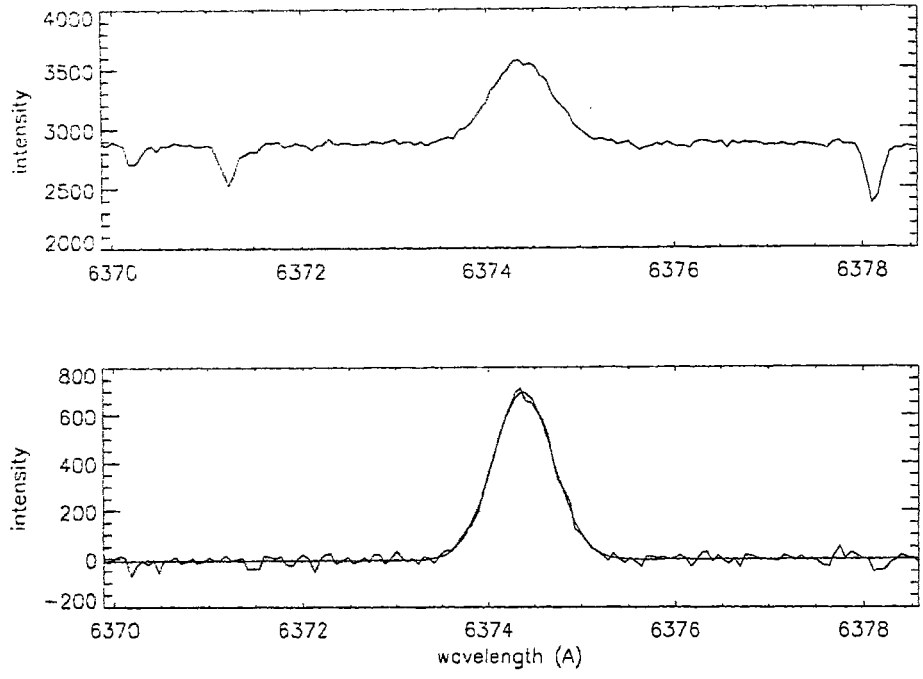

Figure 1. Top panel shows a typical observed profile for the red coronal emission line and bottom panel shows the residual profile after correction for dark current, flat field and scattered light due to sky brightness along with a Gaussian fit to the residual profile.

3. Results

The 6374 Å and 5303 Å line-widths measured during the eclipse experiments indicate that non-thermal velocities of the order of 20 – 30 km s^{-1} need to be invoked to explain the excess observed line-width. The ionization temperature of different ions and temperature of coronal plasma predicts certain line-widths for various coronal emission lines but all the measurements made during eclipses show larger values for line-widths. To determine the existence and cause of non-thermal velocities we have made simultaneous observations using a coronagraph and CCD cameras. The top panel of Figure 3 shows a plot of green line intensity versus red line intensity, the middle panel shows a plot of the FWHM of the green (Δ) and red(*) lines as a function of height above the limb along with the linear fits to the respective data sets, and the bottom panel plot of the intensity ratio (Ig/Ir) against height in arcsec.

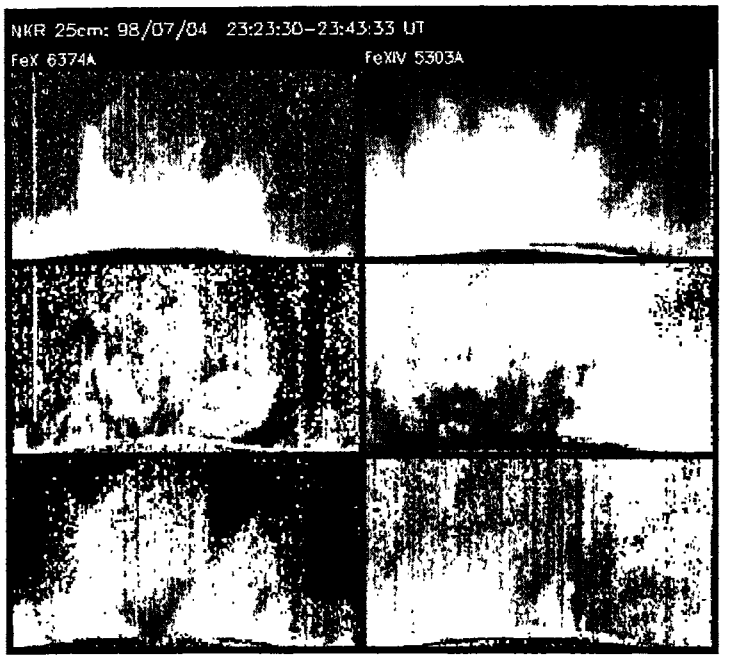

Figure 2. Images of solar corona constructed from the line profiles observed with the 25 cm coronagraph at Norikura Observatory. The top row shows the distribution of the red and green line intensities in the observed coronal region. The middle and bottom rows indicate the velocity and line-width distributions respectively. The range of velocities shown in the gray scale is from −7.0 to +7.4 km s^{-1} for 6374 Å and from −6.3 to 6.4 km s^{-1} for 5303 Å. The line widths in gray scale cover the range 0 – 1.6 Å.

The linear fits to line-widths of the green and red lines shown in the middle panel indicate that the width of the green line decreases with height while that of the red line increases with height above the limb. The bottom panel shows that the intensity ratio Ig/Ir lies between 2 – 10 near the limb and between 1 – 3 at 150″ and that the spread in Ig/Ir values becomes smaller at larger heights.

The top panel of Figure 4 shows a plot of the green versus red line intensities at various locations on an individual structure. The middle panel of the figure shows the variation of FWHM of the red and green lines, marked by (*) and (Δ), respectively, as a function of height above the limb in the coronal structure. The lower panel indicates the variaiton of intensity ratio as a function of height. The straight lines in the top and middle panels of Figure 4 are linear fits to the respective data sets. These figure indicates that in all cases FWHM of the green line decreases with height above the limb while that of the red line increases with height. The slope of linear fit to a plot of Ig verses Ir varies between 1 to 10 for different structures.

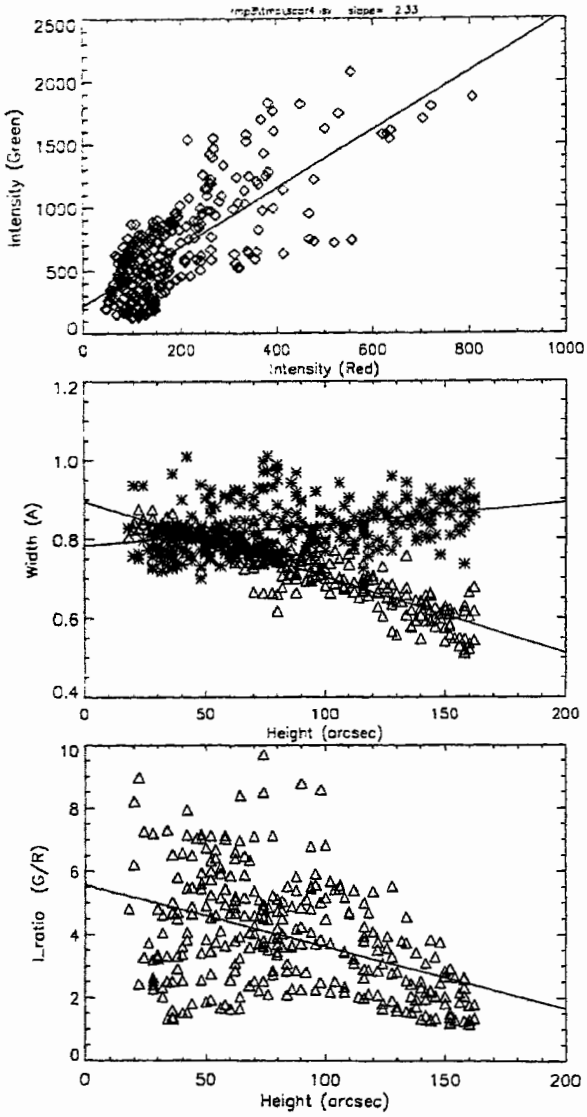

Figure 3. Typical plot made after computing the values of line-width, intensity and velocity over a 4″ × 4″ coronal region by considering all the structures together. Top panel shows the variation of the green line intensity versus red line intensity for a structure observed. Middle panel represents the FWHM of the green (Δ) and red line (*) as a function of height above the limb along with linear fits (straight lines) to the respective data. Bottom panel shows the intensity ratio (Ig/Ir) versus height above the solar limb.

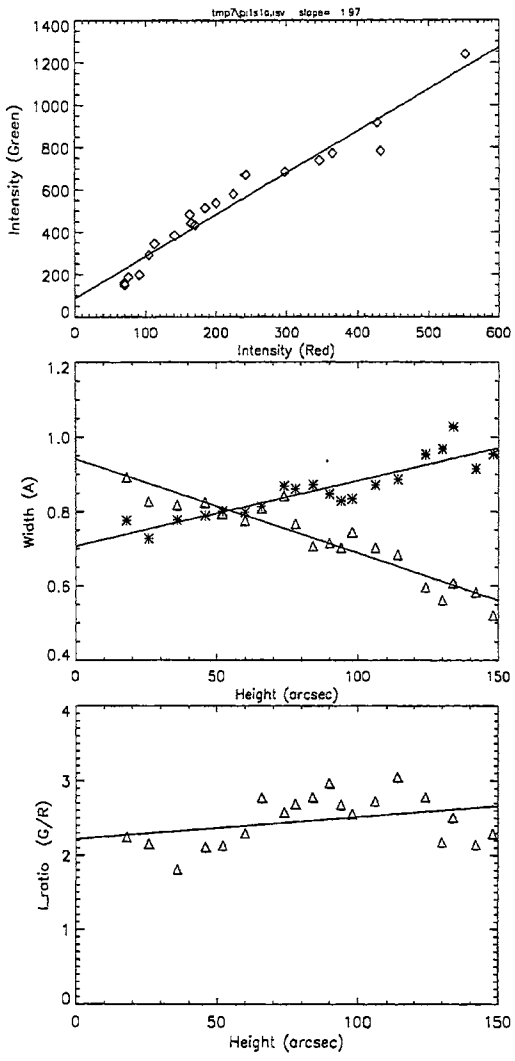

Figure 4. Same as that of Figure 3, but for an individual coronal structure.

4. Discussions

4.1 Intensity ratio and temperature

In general, the intensity ratio of the green to red line (Ig/Ir) is different for different coronal structures and sub-structures. The values of Ig/Ir observed between 0.5 and 14 imply a range of $1.2-1.8\times10^6$ K for the temperature of the coronal structures under investigation (Raju and Singh, 1987). The intensity ratio Ig/Ir is generally greater near the edges of a coronal structure than that in the inner part of the structure and varies with height above the limb along a coronal structure. The value of Ig/Ir increased with height in some structures and decreased in some other coronal structures. In yet other structures the value of Ig/Ir increased up to a certain height and then starts decreasing. It is not possible to explain this complex behaviour in simple terms of diferene in temperature. It may be noted that the variation in the value of Ig/Ir for a structure with height does not involve any large variation in temperature along the structure for most of the coronal structures. In general the intensity ratio (Ig/Ir) lies between 2 – 10 near the limb and between 1 – 3 at heights greater than 100″; the smaller values and spread of the intensity ratio at larger heights may be due to the mixing of plasma by microturbulence at larger heights in the coronal structure in agreement with the findings of Singh et al. (1999).

4.2 Line-width variation with height

In all the structures studied, the FWHM of the green line decreased and that of the red line increased continuously with height above the limb. The values of FWHM for the green line at 50″ and 100″ for different structures show a small range whereas those for the red line show a large range. The mean values for the red line are greater for open sturctures and edges of the structure as compared to the closed structures and inner portions of the coronal structure respectively. In most of the structures the line-widths of both the green and red lines at 50″ increased by small amounts with time; in some structures it varied with irregular interval. The increase in line-width may be due to an increase of temperature or non-thermal velocity.

By averaging over all the structures we get the FWHM of the green and red lines as 0.813 Å and 0.816 Å respectively at 50″ above the limb. Assuming the line-widths are entirely due to thermal braodening the temperature corresponding to these values are 2.57×10^6 K and 1.79×10^6 K respectively, much higher than the ionisation temperatures 1.8×10^6 and 1.0×10^6 K of [Fe XIII] and [Fe IX] ions respectively. We find that the average intensity ratio of the green to red lines is about 5, which corresponds to a temperature of 1.5×10^6 K (Raju and Singh, 1987). Assuming this value for the temperature of these coronal structures, from the above mentioned values of FWHM, we derive the values of non-thermal component of velocity V_t using the following equation

$$\frac{2kT}{M} + V_t^2 = \frac{1}{4\ln 2}C^2\frac{\Delta\lambda^2}{\lambda^2}$$

where T is the coronal temperature, M mass of the ion, c the velocity of light, $\Delta\lambda$ the full width at

half maximum of line profile and λ the wavelength of the coronal emission line. The values thus obtained for non-thermal velocities are 16.8 km s^{-1} and 9.4 km s^{-1} for the green and red lines, respectively.

The average values of FWHM at 100″ over all structures are 0.727 Å and 0.882 Å for the green and red lines, respectively. Assuming $T = 1.5 \times 10^6$ K, we find non-thermal velocities of 12.9 km s^{-1} and 13.2 km s^{-1} for the green and red lines respectively at 100″ above the limb. The average value of non-thermal component of velocity for the green line at 100″ agrees with that for the red line. It may be noted that there may be some variations in temperature at different locations along the coronal structures which have not been taken into account while computing the non-thermal component of velocities.

The averaged values of FWHM at 150″ for the green and red lines are 0.636 ± 0.023 Å and 0.882 ± 0.018 Å respectively. The green line-width corresponds to a temperature of 1.57×10^6 K while the red line-width corresponds to 2.08×10^6 K if we assume that the observed line-width is completely due to thermal broadening. The temperature corresponding to green line-width is less than the ionisation temperature of [Fe XIII] ion whereas that corresponding to the red line-width is much greater than the ionisation temperature of [Fe IX] ion. The computations by Raju & Singh (1987) indicate that ratio (Ig/Ir) of 2 corresponds to a temperature of 1.4×10^6 K. Assuming this to be the real temperature of the top part of the coronal structure we find that the green line-width of 0.636 Å yields a micro-turbulent velocity of 7.3 km s^{-1} and the red line-width of 0.882 Å a value of 14.4 km s^{-1}. The difference in the derived values of non-thermal velocities for the green and red lines may be partly due to a difference in the asusmed and real temperatures of the structure.

The values of ratio of Ig/Ir intensities as a function of height above the limb and computations of micro-turbulence at different heights assuming the temperature corresponding to intensity ratio, indicate that both temperature and micro-turbulence vary in coronal structures as a function of height above the limb. The computed values of non-thermal velocities for both the green and red lines are almost same at 100″ height above the limb.

5. Conclusions

If we assume that non-thermal velocities increase in coronal structure with height as concluded by Doyle, Banerjee & Parez (1998), the width of both the green and red lines should increase with height above the limb, which does not agree with our observations. The monotonic increase or decrease in temperature of coronal structures with height above the limb also cannot explain the observed increase in FWHM of the red line and decrease in FWHM of the green line with height. It is possible to explain the observed behavior if we assume that the fine structures in steady and quiet coronal structures, although they may be broadly guided by magnetic field configuration, are not entirely due to magnetic flux tubes but also due to temperature and density variations within the structures. At the bottom of the coronal structures where the plasma density is high, and perhaps the magnetic field is strong and more concentrated, the contribution to the red line emission comes from a relatively cold plasma and to the green line from a relatively hotter plasma.

It is possible that the hotter plasma surrounds the cold plasma, since the green line structures in our observations appear to be diffused and broad, as compared to structures seen in the red line.

As we move up along the coronal structure, the magnetic field spreads, as indicated by the broadening of structures at larger heights above the limb, the mixing of hotter and relatively colder plasma may occur due to the existence of large thermal and non-thermal velocities. The mixed plasma at large heights may have an average temperature lower than that of the green line plasma, and higher than that of the red line plasma at the bottom of the structure. This process can cause an increase in the FWHM of the red line and decrease in the green line FWHM with height in the coronal structures.

In section 4.2 we have seen that by assuing the coronal temperature derived from intensity ratio at 100″ to represent the real temperature, the non-thermal velocity turns out to be about 13 km s^{-1} for both the green and red lines. The difference in the values of turbulent velocity at 50″ may not be due to non-thermal motions but may be due to a difference in the effective temperature at 50″ in the coronal structure. Similarly, a change in the non-thermal motions can also explain the observed increase and decrease in the red and green line-widths, respectively, with height.

One may also note that FWHM of the green line in both open and closed structures is almost same whereas the FWHM of the red line is more in open structures as compared to the closed loop-like structures. This may be due to the fact that hotter plasma diffuses faster and has similar values of non-thermal velocities both in open and closed field coronal structures, and relatively colder plasma as seen in red line shows larger non-thermal velocities in open structures than in closed coronal structures. The values of FWHM gradient indicate that variations in temperature or turbulence or both are steeper in open coronal structures as compared to those in closed structures.

From the observed variations of Ig/Ir ratios in general and FWHM of both the green and red lines with height above the limb, appears that both temperature and non-thermal velocity vary with height along the coronal structures. Both the temperature and non-thermal velocity decrease when seen in the green line whereas these increase when seen in red line with height above the limb. The fractional change in temperature is marginal as compared to that in the non-thermal velocities.

References

Bessey, R.J., Liebenberg, D.H. 1984, *Sol. Phys.*, **94**, 239.
Chandrasekhar, T., Desai, J.N., Ashok, N.M., Pasachoff, J.M. 1991, *Sol. Phys.*, **131**, 25.
Delone, A.B., Makaraova, E.A. 1969, *Sol. Phys.*, **9**, 116.
Delone, A.B., Makarova, E.A. 1975, *Sol. Phys.*, **45**, 157.
Doyle, J.G., Banerjee, D., Perez, M.E. 1998, *Sol. Phys.*, **181**, 91.
Jarrett, A.H., von Kluber, H. 1955, *Mon. Not. R. Astron. Soc.*, **115**, 343.
Jarrett, A.H., von Kluber,H. 1961, *Mon. Not. R. Astron.Soc.*, **122**, 223.
Liebenberg, D.H., Bessey, R.J., Watson, B. 1975, *Sol. Phys.*, **44**, 345.
Livingston, W. Harvey, J. 1982, *Proc. of INSA, Indian National Science Acad.*, New Delhi, 48A, 18.
Mariska, J.T., Feldman, U., Doschek, G.A. 1978, *Astrophys. J.*, **226**, 698.

Marshall, P.M., Henderson, G. 1973, *Sol. Phys.*, **33**, 153.
Raju, K.P. Desai, J.N., Chandrasekhar, T., Ashok, N.M. 1993, *Mon. Not. R. Astron. Soc.*, **263**, 789.
Singh, J. 1985, *Sol. Phys.*, **95**, 253.
Singh, J., Bappu, M.K.V., Saxena, A.K., 1982, *JApA*, **3**, 249.
Singh, J., Ichimoto, K., Hideki, I., Sakurai, T., Takeda, A. 1999, *PASJ.*, **51**, 269.
Singh, J., Ichimoto, K., Sakurai, T., Muneer, S., 2003, *Astrophys. J.*, **585**, 516.
Singh, J., Sakurai, T., Ichimoto, K., Suematsu, Y., Takeda, A. 2002, *PASJ.*, **54**, 793.
Singh, J., Cowsik, R. (eds.) 1997, *Kodaikanal Obs. Bull.*, Vol. 13.